

Invited Paper

Multifunctional photonic devices based on polymeric materials

Gauri Karve^a, Bipin Bihari^a, Dechang An^a, Suning Tang^b, Ray T. Chen^a

^aMicroelectronics Research Center, University of Texas, Austin, TX 78758

^bRadiant Research Inc., 9430 Research Blvd., Suite IV305, Austin, TX 78759

ABSTRACT

A multifunctional polymeric device capable of performing functions such as electro-optic modulation, optical amplification, and electro-optic switching simultaneously is described. All three modules can be built on a single substrate. A novel polymeric modulator with structure based on 1x2 Y-fed directional coupler is demonstrated. The results of preliminary investigations on optical amplifiers are presented.

Keywords: Photonic IC, Optical amplifiers, Electro-optic modulators, Rare earth ions, polymers, chromophores, electro optic coefficient

1. INTRODUCTION

As Si CMOS device speeds increase, the overall circuit delay is determined by the inter-chip signal transmission time. It is necessary to have fast signal transport between the processing elements, memories and other peripheral devices. Conventional interconnect speeds are limited by RC time delays. The alternative ways for high speed data transmission are needed. The use of optical interconnects is the most promising solution. For realizing the optoelectronic interconnects, efficient and cost-effective modules for electro-optic modulation, switching, wavelength conversion, optical amplification, etc. need to be investigated. A multifunctional photonic integrated circuit is suitable for such tasks.

Several crystalline materials, like LiNbO₃ and III-V compound semiconductors have been extensively investigated for multiple functions such as modulation, switching, wavelength conversion and amplification. However, these systems have several disadvantages. Single crystal materials exhibit sharp and polarized absorption and emission lines¹. Hence they are not very useful as optical gain media unless polarization converters are used². These materials are also strictly substrate-selective due to required lattice-matching for single crystal thin film growth. Finally, the fabrication costs associated with these materials are very high.

Polymeric optical materials, on the other hand, have no above-mentioned shortcomings³. Polymeric material systems can easily be engineered to change their microstructure to provide various optical parameters such as bandwidth of transparency, high values of r_{33} , temperature stability, etc. for specific applications. They are usually in a glass state that can provide a wider bandwidth of amplification if an appropriate gain mechanism is identified. The polymer fibers are lightweight and have good ductility. It is easy to splice them to each other and to the light source due to their large core diameter and high numerical aperture. They are relatively insensitive to vibrational stress, have large flexibility and are easy to process. Therefore, it is ideal to combine the advantages of polymeric materials and their non-linear properties with the gain of rare-earth-doped polymers⁴ to produce amplifiers. Further, transferability of polymer thin films onto different substrates of interest is an added advantage.

A polymer-based integrated optical module containing, electro-optic modulator, electro-optic switching device and optical wavelength conversion/amplifier is under development. Fig. 1 shows the design of this multi-functional module. Such device module is proposed for the first time in polymer-based photonic integrated circuits. It can be built on a single substrate. This cascaded 2x2 switch has independent addressability and a post-modulation gain control. Section I of the

module converts electrical signal to optical signal. Section II is for the electro-optic switching. In section I and II, index modulation is achieved. These two sections are doped with electro-optic chromophore within which index is modulated through an external electric field. Section III is the amplification region. It is doped with suitable rare-earth-ions. The pump beam of wavelength λ_2 , needed for optical amplification, travels in two separate channel waveguides and is introduced in the gain region through directional couplers. The pump beam propagates collaterally with the signal beam λ_1 and amplifies the signal⁴. These modules are being studied individually. A rare earth ion doped amplifier and an electro-optic modulator are described in the following sections.

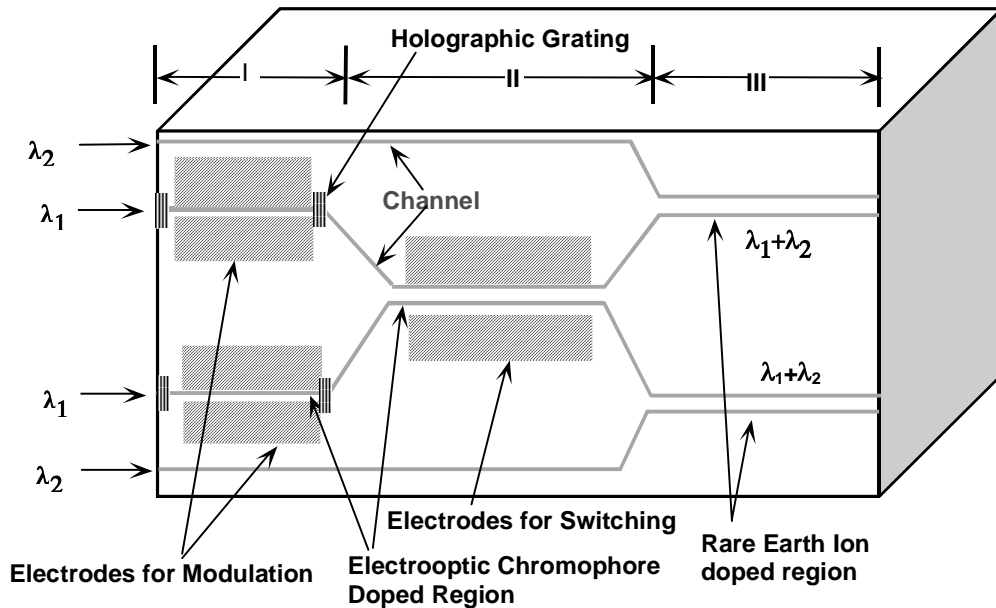


Figure 1. Multi-functional guided wave module with modulation, switching and amplification.

2. OPTICAL AMPLIFIERS

Amplifiers are needed to account for various losses in the system or the intensity decrease due to splitting of the signal. The losses could be due to scattering and/or absorption in the medium, imperfect coupling and de-coupling, mismatch between the laser mode and waveguide mode, etc.

Organic dyes and rare earth ions have been used as dopants to achieve amplification at various wavelengths. Gain of about 37 dB/m at 580 nm has been demonstrated in an organic dye, Rhodamine B, doped poly(methylmethacrylate) (PMMA) optical fiber⁵. However, photostability is a serious problem for an organic dye doped polymer. Rare earth elements have also been used extensively as active ions in amplifiers and lasers. Their electronic configuration is $[Xe] 5d 6s^2$ plus a certain number (1-14) of 4f electrons. The outer 5d and 6s electrons shield the inner 4f electrons. As a result of this, the 4f energy levels are relatively insensitive to host and are weakly mixed with the higher energy levels. The observed visible and infrared spectrum of trivalent rare earth ions is a consequence of transitions within these 4f states. This makes rare earth ions attractive candidates for lasing and amplification applications. Sensitized excitation of the rare earth ions is also possible⁶. Sensitized excitation of Nd^{3+} ions is under consideration. In indirect excitation, the active ions are excited through the ligand attached to them. The pumping efficiency could be higher in this case if the absorption cross-section of the ligand is high. It also gives flexibility in choosing the pump wavelength.

Extensive research on rare-earth doped fiber lasers and amplifiers in the past few years has led to the development of a myriad of active devices^{7,8}. In particular, the Er^{3+} doped fiber amplifiers (EDFA) operating at 1.55 μm have reached a stage of practical applications for optical telecommunications⁹. Along with the inorganic rare earth compounds as dopants, organic compounds like rare earth chelates, especially β -diketones of rare earth ions have also been used for doping the silica

fiber¹⁰. Incorporation of β -diketones of rare earth ions in polymers has also been demonstrated. Gain of about 2.7 dB/cm at 615 nm has been established in a Eu(III) hexafluoroacetylacetonate (Eu(HFAA)) doped poly(lauryl methacrylate) (PLMA)¹¹. Superfluorescence has been observed in Eu(III) hexafluoroacetylacetonate doped poly(methylmethacrylate) (PMMA) fiber⁵. A similar Nd compound, (Nd(III) hexafluoroacetylacetonate), for amplification at 1.06 μm has been used for doping a polyimide matrix. Photoluminescence from Nd^{3+} ions in this system has been studied¹². The amplified spontaneous emission by deuterated hexafluoroacetylacetonate Nd(III) or Eu(III) in a PMMA and P-FIPMA (polyfluoroisopropylmethacrylate) matrix has been shown to have quantum yields as high as 72%¹³ for Eu(III) hexafluoroacetylacetonate in P-FIPMA system.

We have demonstrated gain of about 3.8 dB/cm at 1.06 μm in NdCl_3 doped photolime gel polymer with a planar waveguide geometry¹⁴. Photolime gel has a glass transition temperature between 110°C and 135 °C. Hence the maximum temperature reached during the processing of the waveguide should be below this temperature. This makes difficult to remove the water contamination from the system completely. Hydroxyl groups strongly absorb radiation in the near-IR regime¹⁵. This leads to a decrease in the signal output, and the device does not have long term stability. A similar observation was made in the system of ErCl_3 doped photolime gel for amplification at 1.55 μm ¹⁶.

In order to overcome problems associated with photolime gel, we considered polyimide as host material. Polyimides are widely used for electronic packaging. Further, their high glass transition temperature (nearly 400°C) makes them compatible to high temperature processing of Si-CMOS devices. They are moisture insensitive and are resistant to many organic solvents. Polyimides, particularly fluorinated polyimides have very low optical loss. Loss as less as 0.3 dB/cm has been reported¹⁷. We have used a fluorinated polyimide, Ultradel 9120, available from Amoco Chemicals. The polymer has a refractive index of about 1.523 at 1.33 μm . Amongst rare earth elements, we used Neodymium (Nd) compounds to obtain amplification at 1.06 μm . Nd chelates and Nd inorganic compounds are being studied. A simple way to dope polyimide with RE ions is to dissolve both the RE compound and the polyimide in a common solvent or in two different miscible solvents and then spin coat the mixture to get a thin film which is a planar waveguide. As polyimide, we use, is a photosensitive polymer (acts like a negative photoresist), thin films can be patterned easily using UV exposure to get a channel waveguide.

Among the several rare earth chelates considered, Nd(III) hexafluoroacetylacetonate (Nd(HFAA)) and Nd(III) acetylacetonate (NdAA) were found to have good solubility in γ -butyrolactone (standard solvent for polyimide). With Nd(HFAA), solubility upto 0.18 M could be obtained easily. This high solubility makes it easy to achieve high Nd^{3+} concentration in the mixture. However, NdAA is hygroscopic and decomposes in water, making it relatively difficult to handle. Further, γ -butyrolactone is not a good solvent for Nd(III) trifluoromethylsulfonate (Nd(TFMS)) and Neodymium chloride hexahydrate ($\text{NdCl}_3 \cdot 6\text{H}_2\text{O}$). Therefore, 1-Methyl-2-pyrrolidone (NMP) was used as a solvent for $\text{NdCl}_3 \cdot 6\text{H}_2\text{O}$.

Non-radiative energy transfer is the main route of deactivation of the excited Nd^{3+} states. The harmonic oscillators in the system with the energy of vibrational quanta greater than or equal to the energy gap of the radiative transition states are capable of quenching the excited Nd^{3+} states¹⁵. The energies of second harmonics of C-H and O-H vibrational stretch match closely with the energy difference of 1.06 μm -radiative transition in Nd^{3+} (corresponding to ${}^4\text{F}_{3/2} \rightarrow {}^4\text{I}_{11/2}$ transition). This enhances the thermal deactivation and decreases the radiative lifetime of the excited states of Nd^{3+} ions. One way to overcome this problem is to fluorinate or deuterate the compound. Quenching of the excited Nd^{3+} ions by C-F and C-D oscillators is due to their third and fifth harmonics respectively instead of the second. Hence, the probability of non-radiative energy transfer is less in this case. Correspondingly, the radiative life time of the excited states of Nd^{3+} ions is increased. Thus, we expect NdHFAA to be a better candidate than NdAA for amplification. However, fluorination of the compound tends to decrease the intermolecular attraction and the compound becomes more volatile. Processing polyimide involves baking at relatively high temperatures and hence the problem is even more serious. Sublimation of Nd(III) hexafluoroacetylacetonate in polyimide and subsequent loss in the photoluminescence signal has been observed¹². Use of such compounds might still be possible if a low temperature processing is used for polyimide. We are studying inorganic Nd^{3+} compounds that have lower vapor pressures and higher melting points.

For making thin films of the doped polyimide, the mixture of solvent, Nd compound and polyimide was spin coated on a glass, quartz or Si with SiO_2 substrate. The film thickness was controlled by changing spin speed and time. Ultradel 9120 processing requires baking at temperatures as high as 250°C. This doesn't create any problem for Nd chloride dopant as hydrated NdCl_3 ($\text{NdCl}_3 \cdot 6\text{H}_2\text{O}$) loses all its water molecules at about 150°C and is stable after that. However, melting point of NdHFAA is nearly 150-155 °C. Hence the processing conditions need to be manipulated. Sihan Lin, et al. have studied low temperature processing of NdHFAA in polyimide matrix¹². Following those lines, after spin coating, the sample was first soft baked at 100°C on a hot plate for about 6 min in air to remove the solvent molecules and the water molecules. The

sample is then exposed to UV light. The typical dosage is 1000-1500 mJ/cm². This is to photocrosslink the polymer. The sample was then baked at 175°C for 30 min in a N₂ purged oven. This final bake is needed to remove the solvent completely and to improve the fine features of the film.

1.1. Photoluminescence Experiment

The photoluminescence(PL) from the Nd³⁺ ions incorporated in the polyimide matrix was studied. In order to increase the interaction volume and hence the fluorescence signal strength, thick samples were used. A hemispherical drop of the doped polymer about 1 cm in diameter was placed on a glass substrate and processed directly without spin coating. The soft bake time and the UV exposure time were increased to facilitate complete drying and photo-crosslinking of the sample. The final hard bake was done at 175°C for about 30 min in a N₂ purged oven. The Nd³⁺ ions were excited using an Ar ion laser at wavelength 488 nm. The typical pump power used was 100 mW. The PL signal was collected using a lens in front of the sample. The signal was then passed through a grating spectrometer and was detected using a N₂ cooled Ge detector.

The PL signal obtained for Nd(III) hexafluoroacetylacetonate doped polyimide is shown in Fig. 2. A characteristic PL signal corresponding to ⁴F_{3/2} → ⁴I_{11/2} transition is observed at 1.056 μm. The FWHM of the peak is 0.0225 μm. This is large compared to that observed for PL emission by Nd³⁺ ions in crystalline inorganic hosts⁷. This is mainly due to the amorphous nature of the polymer host. The number density of Nd³⁺ ions in the sample was nearly 5x10¹⁹ ions/cc of polyimide. Sihan Lin, et al. have also done the photoluminescence studies of Nd(III) hexafluoroacetylacetonate doped polyimide¹². Our results compare well with their findings.

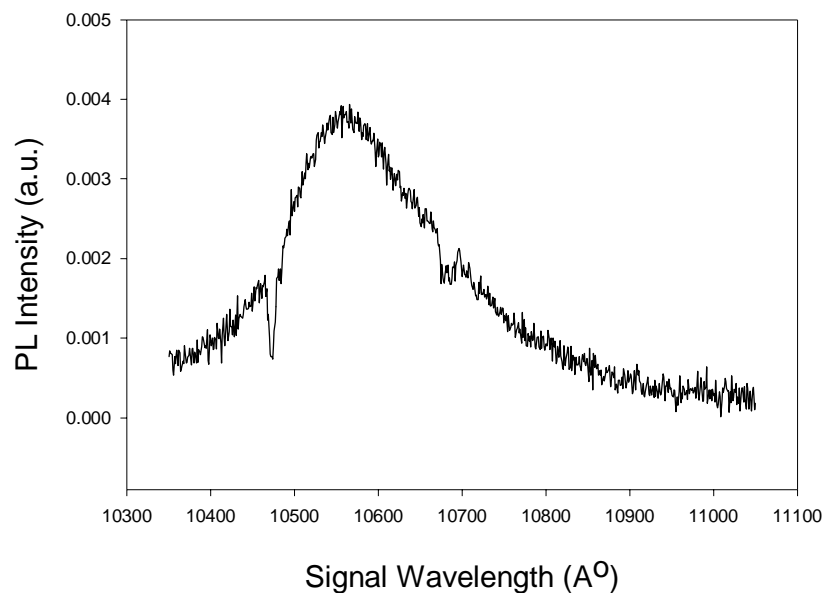


Figure 2. PL signal as a function of signal wavelength for Nd(III) hexafluoroacetylacetonate doped polyimide at 1.06 μm.

1.2. Experimental Setup for Optical Gain Measurement

Fig. 3 shows the experimental set up for studying the optical amplification in a planar waveguide. The pump beam and the probe beam were coupled into the planar waveguide using prism coupling technique. Both P₁ and P₂ are glass prisms of refractive index higher than that of the film. The prism P₁ is also used to de-couple the probe beam. The pump beam and the probe beam counter-propagate in the film. A good overlap between these two beams should be ensured in order to have an efficient transfer of energy from the pump to the probe beam. OD₁ and OD₂ are the optical neutral density filters used to control the pump and the probe beam intensity. The amplified 1.06 μm signal is then passed through a rejection filter F₁ and a band pass filter F₂, both working at 1.06 μm and is then detected using a Newport Ge photodetector. A tunable Ti-Sapphire laser is used to pump Nd³⁺ ions at 800 nm or 745 nm. Nd-YAG laser emitting at 1.06 μm is used as the probe beam. Another

geometry where the pump and the probe beam co-propagate is also possible. The ease of having a good overlap between the pump and the probe beams is an advantage in this case.

For an amplifier consisting of $\text{NdCl}_3 \cdot 6\text{H}_2\text{O}$ doped photolime gel, a gain of about 3.8 dB/cm was observed¹⁴. The gain was seen to be strongly dependent on the Nd^{3+} ion concentration (see Fig. 4), dropping off sharply at high concentrations due to concentration quenching. Fig. 5 shows the pump power dependence of the gain. The gain saturates at pump powers over 200 mW. The pump wavelength dependence shows a maximum in the output at the absorption wavelengths of Nd^{3+} ions as expected. The interaction length dependence and probe beam intensity dependence (Fig.6) has also been studied.

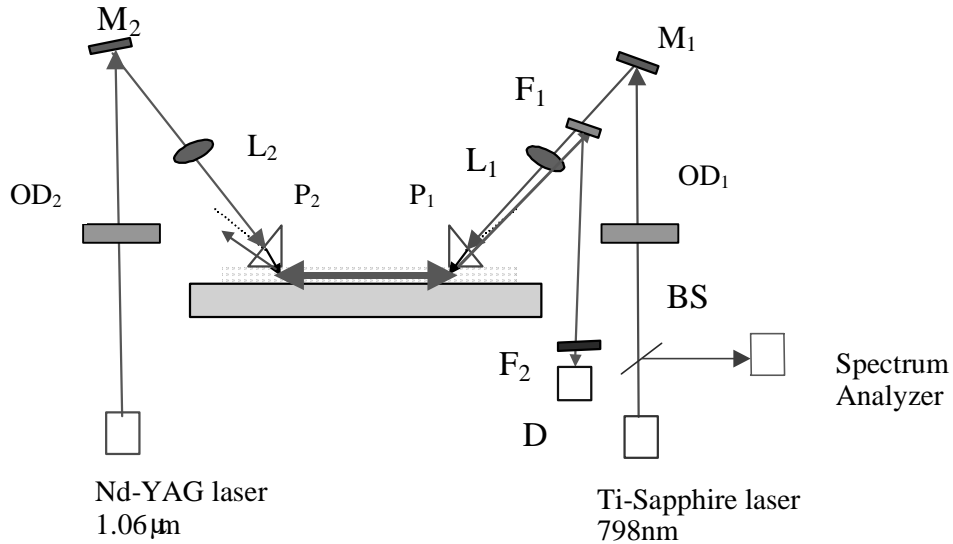


Figure 3. Schematic of the set up for gain measurement.

L_1, L_2 : Focussing lens, M_1, M_2 : Mirror, F_1 : Rejection filter, F_2 : Bandpass filter, BS: Beam Splitter, D: Detector, OD_1, OD_2 : Optical neutral density filters

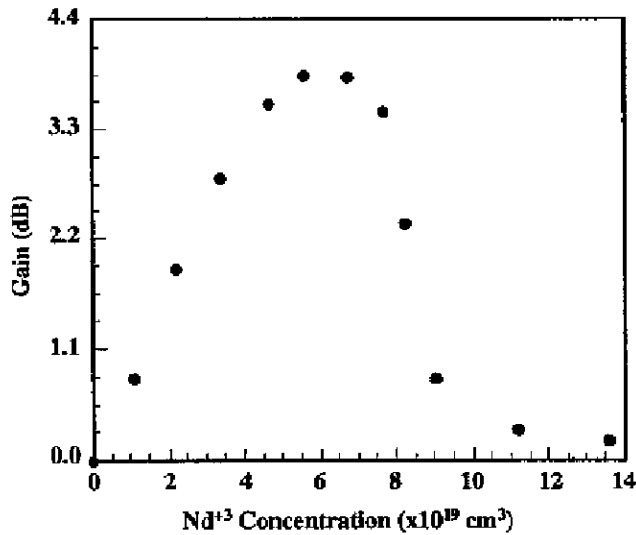


Figure 4. Dependence of gain on Nd^{3+} concentration in a $\text{NdCl}_3 \cdot 6\text{H}_2\text{O}$ doped photolime gel

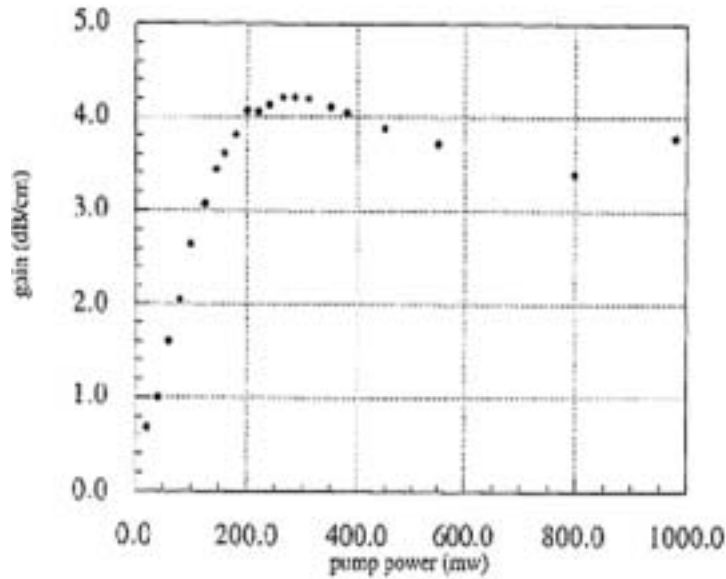


Figure 5. Dependence of gain on pump power in $\text{NdCl}_3 \cdot 6\text{H}_2\text{O}$ doped photolime gel

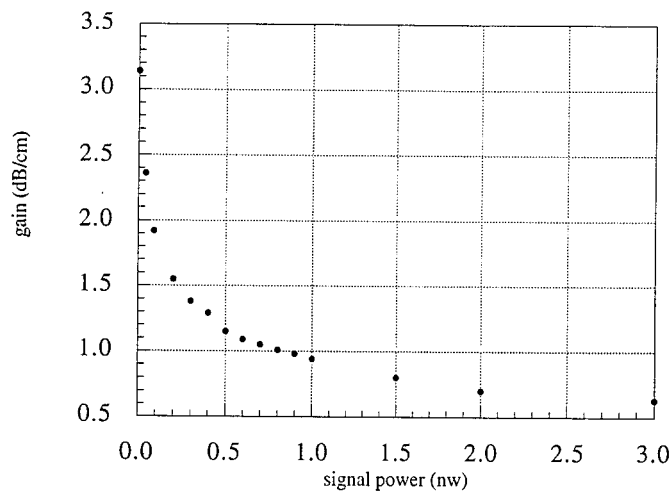


Figure 6. Dependence of gain on signal power in $\text{NdCl}_3 \cdot 6\text{H}_2\text{O}$ doped photolime gel

3. Electro-optic Modulator

Electro-optic modulators have important applications in optical communication, phase array antennas, and sensing systems^{18,19,20}. Inorganic crystal (such as LiNbO_3) based modulators are commercially available. However, further improvement of inorganic modulators in high-speed scenario is restricted severely due to large phase velocity mismatch between the guided optical signal and the modulating microwave signal^{21,22}. Electro-optic polymers have several intrinsic advantages over inorganic crystals. They have higher electro-optic coefficients, reduced phase velocity mismatch, and flexibility of device fabrication. Several EO polymer based Mach-Zehnder modulators have been demonstrated recently^{23,24,25}. However, the device structure tends to be complicated for a Mach-Zehnder modulator, due to the requirement of applying a DC bias to set the modulator at the half-power point. Further, the DC drift phenomena often causes distortion in its modulation linearity^{26,27}. Only a few polymeric modulators with other structural configurations have been investigated.

Here, we demonstrate a polymeric modulator based on a 1x2 Y-fed directional coupler structure. Simple waveguide structure employed here offers the modulator several unique operating characteristics. As shown in Fig.7, the modulator consists of two parts--a single-mode Y-junction for feeding light in, and a co-directional coupler having a pair of parallel and symmetric single-mode waveguides. The traveling-wave electrodes are fabricated over the coupler waveguides, and the two output-ends are connected with optical fibers for packaging.

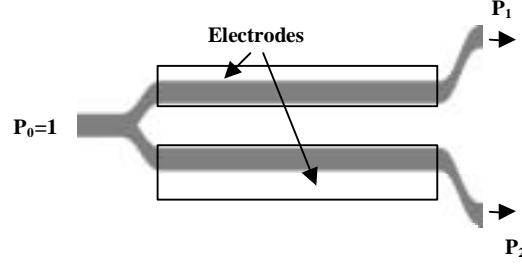


Figure 7. Schematic of 1x2 Y-fed coupler modulator with travelling-wave electrodes on top. The input intensity is unity.

The Y-fed modulator is characterized by, the interaction length L (equal to the electrode length), the coupling coefficient κ or the coupling conversion length ($l_c = \pi/2\kappa$), which is the minimum length required to obtain complete crossover of optical power from one branch to another and the electro-optically induced mismatch in the propagation constants ($\Delta\beta = \beta_1 - \beta_2$) of the two waveguides, when a driving field is applied. For a push-pull structure, we have

$$\Delta\beta = \frac{2\pi}{\lambda} n_e^3 r_{33} \alpha \frac{V}{d} \quad (1)$$

where λ is the wavelength of light, n_e is the extraordinary index of refraction for EO film, d is the electrode spacing, and α is the overlap integral between the applied electrical field and the optical field ($0 < \alpha < 1$). For unit input light intensity, the output optical power P_1 of the top waveguide can be calculated using the coupled-mode theory^{28,29} as

$$P_1 = \frac{1}{2} \left[1 - \frac{2xy}{r^2} \sin^2 \left(\frac{\pi r}{2} \right) \right] \quad (2)$$

The output power in the lower arm is $P_2 = 1 - P_1$

Here,

$x = \Delta\beta L / \pi$, normalized driving voltage;

$y = L / l_c$, normalized interaction length;

and $r^2 = x^2 + y^2$.

x is a linear function of the applied voltage, i.e. $x = \Delta\beta L / \pi = K_1 V$, K_1 is a constant depending on the geometry of the optical waveguides and the electrodes, the refractive index and the electro-optic coefficient of the polymer. According to Equation (2), the 1x2 Y-fed coupler modulator is set at the 3dB operation point automatically, i.e. $P_1 = P_2 = 1/2$ when $V = 0$. Under the action of the driving voltage, light can be coupled from one channel into another. Fig. 8 shows the calculated output intensity as a function of normalized driving voltage, for $y = 0.5, 1/\sqrt{2}, 1.5$ and $2/\sqrt{2}$. Note that the modulator functions as an optical switch, shifting between on and off states or the so called "cross-over" and "bar" states when $y = L / l_c = (2n + 1) / \sqrt{2}$ ($n = 0, 1, 2, \dots$). In our design, $L / l_c = 1 / \sqrt{2}$ for a compact device with minimum driving voltage corresponding to a 100% modulation depth is used. It is possible to improve the linearity and of modulation and reduce distortion further by employing domain-inverted poling technique and multi-section electrodes^{30, 31}.

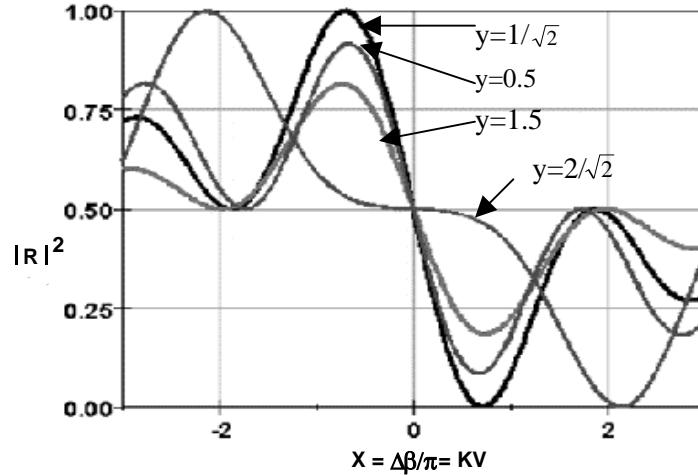


Figure 8. Modulated light intensity as a function of normalized driving voltage for various y values.

The EO polymer used in this experiment is a thermo-setting polyurethane crosslinked with a chromophore called FTC. The chromophore FTC is based on a tricyanobutadiene acceptor incorporating a furan-derivative ring. With this novel chromophore, an EO coefficient over 50 pm/V was obtained in a guest-host polymer system. Polyurethane is well known to enhance the thermal stability and UV sensitivity of the polymer. During the poling of the EO film at an elevated temperature, the crosslinking networks are formed with the EO chromophore in the present of a crosslinker. Detailed information concerning the synthesis and the poling process of this material system will be reported elsewhere.

A cross-sectional schematic of the device is shown in Fig. 9. A 0.2 μm thick layer of gold was deposited by electron beam evaporation method on a silicon wafer. This gold layer acts as the ground electrode. A 100 \AA thick layer of chromium was used to improve the adhesion of Au to Si wafer. The bottom cladding was a 3 μm thick layer of commercially available Epoxylite 9653-2 ($n=1.54$ @ 1.31 μm). To fabricate the EO polymer layer, a pre-polymer was synthesized using FTC chromophore and the monomers of polyurethane. A solution of this pre-polymer and a crosslinker (triethanolamine) was spin-coated on the bottom cladding layer. After drying the sample in a nitrogen-purged oven at room temperature, the EO film was poled using corona poling method. The typical needle-to-plane distance was ~ 2 cm. A DC voltage of 5-6 kV was applied, which resulted a poled circular area, 3 cm in diameter. During the thermal-setting and poling process, the sample was pre-cured at 120 $^{\circ}\text{C}$ for about 3 min and then kept for one hour at 100 $^{\circ}\text{C}$. The sample was then cooled down to room temperature with the poling voltage on. The refractive index of the EO film was 1.65 for TM mode. The propagation loss was found nearly 0.6 dB/cm at 1.31 μm wavelength.

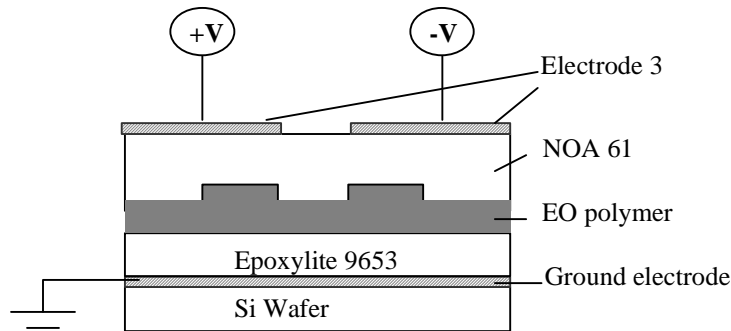


Figure 9. Cross-sectional view of the device. Channel width = 6 μm , channel separation=6 μm , rib step=0.3 μm .

The Y-fed waveguide channels were fabricated using oxygen plasma etching (RIE) technique. To get a smooth polymer waveguide channel with low scattering loss, the RIE etching parameters such as pressure, RF power, oxygen flow flux, and etching time were optimized experimentally. The thickness of original EO film was 2 μm before etching. The etched waveguide rib was 0.3 μm high and 6 μm wide. After removing the residual photoresist, a 3 μm thick layer of NOA61 ($n=1.54$ @ 1.31 μm , from Northland Corp.) was spin-coated as top cladding. The top electrodes (1.5cm long) were patterned using

photolithography and wet etching technique. Note that all the processes were carried out at room temperature, to avoid any damage to EO polymer. Two bonding pads UV15 ($n=1.51$ @ $1.31\mu\text{m}$) were attached to either ends of the waveguide channels to protect the lubricant (DI water) from osmosis and damage during polishing. Finally, the sample was diced and polished for testing.

For photo-testing, a laser beam of $1.31\mu\text{m}$ wavelength was coupled into the device using a 40X objective. Another 40X objective was used to collect the output light. The output light was detected using high-speed photo-detector and Spiricon IR camera. It was found that TE mode light had a higher propagation loss than TM mode. Fig. 10 shows the output of both the waveguides with modulating voltages of 0 V and 9 V, respectively. The modulation curves of the device displayed on an oscilloscope are shown in Fig. 11. To test the stability of the modulator, it was operated at a laser input of 70mW at $1.31\mu\text{m}$ over 400 hours. No decrease in the efficiency was observed during this period.

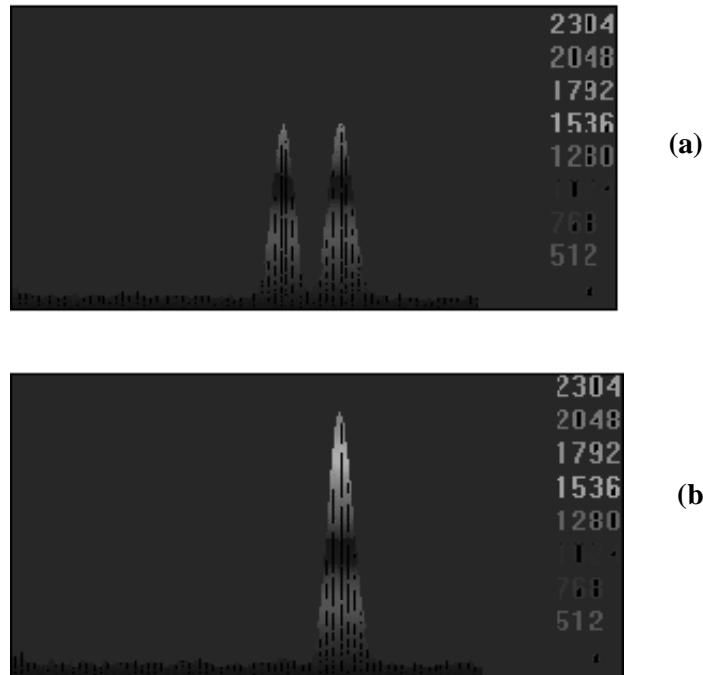


Figure 10. Light intensity throughout of the two waveguide of the modulator when driving voltage is (a) 0V; (b) 7V.

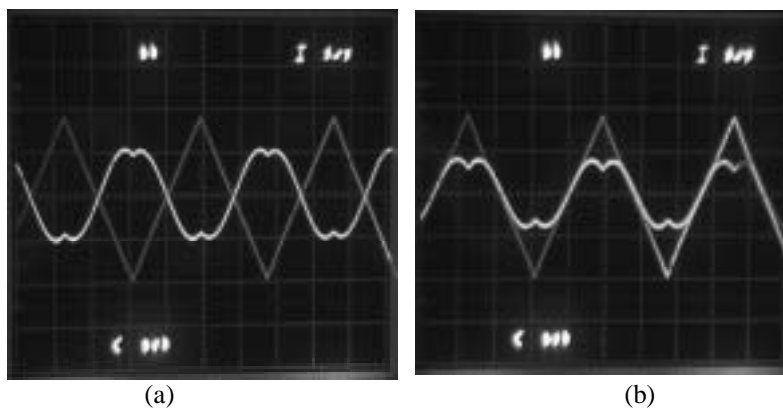


Figure 11. Modulation curves displayed on oscilloscope. The triangular waveform is of the modulating voltage and the sinusoidal waveform is the output. (a) upper waveguide; (b) lower waveguide.

3. CONCLUSION

A polymer based photonic integrated circuit is described. It can be built on a single substrate and is capable of electro-optic modulation, electro-optic switching and optical amplification. Photoluminescence from Nd(III)hexafluoroacetylacetonate doped polyimide is observed. Results of our preliminary investigations suggest that β -diketones of Nd ions and inorganic Nd compounds are promising candidates as active dopants for amplification at 1.06 μm . An electro-optic modulator based on 1x2 Y-fed directional coupler structure is demonstrated. The modulator is set to 3 dB operating point intrinsically due to this design. The electro-optic polymer system is synthesized by crosslinking polyurethane with chromophore FTC. EO coefficient of 19 pm/V is achieved at 1.33 μm . The modulator is driven into optical switching at 3.6V with an extinction ratio of 26 dB.

ACKNOWLEDGEMENTS

This work is supported by DARPA, BMDO, and Office of Naval Research.

REFERENCES

-
- 1 T. Y. Fan, A. Cordova-plaza, M. J. F. Digonet, R. L. Byer, and H. J. Shaw, "Nd:MgO:LiNbO₃ continuous wave laser devices", *J. Opt. Soc. Am B3*, 140-147, 1988.
 - 2 E. Lallier, "Rare-earth-doped glass and LiNbO₃ waveguide lasers and optical amplifiers", *Appl. Opt.*, **31**(25), pp. 5276, 1992.
 - 3 R. T. Chen, "Polymer-based photonic integrated circuits", *Optics and Laser Tech.*, **25**(6), pp.347-365, 1993.
 - 4 R. T. Chen, M. Lee, S. Natarajan, C. Lin, Z. Z. Ho and D. Robinson, "Single-Mode Nd³⁺-Doped Graded-Index Polymer Waveguide Amplifier," *IEEE Photonics Technology Letters*, **5**, pp. 1328-1331, 1993.
 - 5 T. Kobayashi, K. Sasaki, Y. Koike, "Polymer optical fiber amplifiers for communication and sensor applications", *SPIE*, **3281**, pp. 84-91, 1998.
 - 6 M. H. V. Werts, J. W. Hofstraat, F. A. J. Geurts, Jan W. Verhoeve, "Fluorescein and eosin as sensitizing chromophores in near-infrared luminescent ytterbium(III), neodymium(III) and erbium(III) chelates", *Chem. Phys. Lett.*, **276**, pp. 196-201, 1997.
 - 7 M. J. F. Digonet, *Rare Earth Doped Fiber Lasers and Amplifiers* (Marcel Dekker, Inc., 1993).
 - 8 E. Snitzerm C. J. Koester, "Amplification in a fiber laser", *Appl. Optics*, **3**, pp. 1182-1186, 1964.
 - 9 R. Chen, "Holographic Elements Fanout Laser Beams," *Invited Paper to Laser Focus World*, pp. 1-4, 1996.
 - 10 R. P. Tumminelli, B. C. McCollum, E. Snitzer, "Fabrication of High-Concentration Rare-Earth Doped Optical Fibers Using Chelates", *J. Lightwave. Tech.*, **8**(11), pp.1680-1683, 1990.
 - 11 P. K. Sharma, A. R. Van Doorn, E. C. J. Staring, "Optical gain in rare earth doped polymer amplifiers" *Proceedings of Plastic Optical Fibres and Applications*. pp. 115-117, 1993.
 - 12 Sihan Lin, R. J. Feuerstein, A. R. Mickelson, "A study of neodymium-chelate-doped optical polymer waveguides", *J. Appl. Phys.*, Vol. **79**(6), pp.2868-2874, 1996.
 - 13 Y. Hasegawa, k. Sogaba, Y. Wada, T. kitamura, N. Nakashima, S. Yanagida, "Enhanced Luminescence of Lanthanide(III) Complex in Polymer Matrices", *Chem. Phys. Lett.*, **248**(1-2), pp. 8-12, 1996.
 - 14 Dechang An, Zuzhou Yue, Ray t. Chen, "Dual-functional polymeric waveguide with optical amplification and electro-optic modulation", *Appl. Phys. Lett.*, **72**(22), pp. 2806-2808, 1998.
 - 15 Y. Hasegawa, K. Murakoshi, Y. Wada, S. Yanagida, J-H. Kim, N. Nakashima, T. Yamanaka, ' Enhancement of luminescence of Nd³⁺ complexes with deuterated hexafluoroacetylacetonato ligands in organic solvent", *Chem. Phys. Lett.*, **248**, pp.8-12, 1996.
 - 16 K. Spariosu, D. Robinson, P. Low, Z. Z. Ho, S. syracuse, "Erbium-doped polymer waveguide amplifiers", *SPIE*, **3135**, pp.79-85, 1997.
 - 17 T. C. Kowalczyk, T. Kosc, K. D. Singer, P. A. Cahill, C. H. Seager, M. B. Meinhardt, A. J. Beuhler, D. A. Wargoski, " Loss mechanisms in polyimide waveguide", *J. Appl. Phys.*, **76**(4), pp. 2505-2508, 1994.
 - 18 R. C. Alferness, *Integrated Photonics Research*, **7**(L2-1), 1995.
 - 19 P. R. Ashley, Proc. *SPIE*, **2290**, pp. 114-124, 1994.
 - 20 R. C. Alferness, *IEEE Trans. Microwave Theory Tech.*, **MTT-30**(8), pp. 1121, 1982.

-
- ²¹ K. Noguchi, O. Mitomi, K. Kawano, and M. Yanagibashi, *IEEE Photonics Technology Letters*, **5**(1), pp. 52, 1993.
- ²² J.H. Schaffner, J.F. Lam, C.J. Gaeta, G.L. Tangonan, R.L. Joyce, M.L. Farwell and W. Chang, *IEEE Photonics Technology Letters*, **6**(2), pp. 273, 1994.
- ²³ D. Chen, D. Bhattacharya, A. Udupa, B. Tsap, H.R. Fetterman, A. Chen, S.S. Lee, J. Chen, W. H. Steier, and L.R. Dalton, *IEEE Photonics Technology Letters*, **11**(1), pp. 54, 1999.
- ²⁴ Y. Shi, W. Wang, J. H. Bechtel, A. Chen, S. Garner, S. Kalluri, W.H. Steier, D. Chen, and H.R. Fetterman, *IEEE J. Sel. Top. Quantum electron.*, **2**, pp. 289, 1996.
- ²⁵ T. A. Tumolillo, P. R. Ashley, *Appl. Phys. Lett.*, **62**(24), pp. 3068-1070, 1993.
- ²⁶ Y. Shi, W. Wang, W. Lin, D.J. Olson, and J.H. Bechtel, *Appl. Phys. Lett.*, **71**(16), pp. 2236, 1997.
- ²⁷ H. Park, W. Hwang, and J.J. Kim, *Proc. SPIE*, **2852**, pp. 286, 1996.
- ²⁸ H. Kogelnik, R. Schmidt, *IEEE J. Quantum Electron.*, QE-**12**, pp. 396-401, 1986.
- ²⁹ S. Thaniyavarn, *Electron. Lett.*, **22**, pp. 941-942, 1986.
- ³⁰ D. An, S. Tang, Z. Yue, J. Taboda, L. Sun, Z. Han, X. Lu, R. T. Chen, *SPIE*, **3632**, pp. 220-231, 1999.
- ³¹ R. F. Tavlykaev, R. V. Ramaswamy, *J. Lightwave Tech.*, **17**(2), pp. 282, 1999.